Original article

Lipocalin 2 attenuates iron-related oxidative stress and prolongs the survival of ovarian clear cell carcinoma cells by up-regulating the CD44 variant

Running title: Role of LCN2 in ovarian carcinoma

Yasushi Yamada, M.D., Tsutomu Miyamoto, M.D., Ph.D., Hiroyasu Kashima, M.D., Ph.D., Hisanori Kobara, M.D. Ph.D., Ryoichi Asaka, M.D., Hirofumi Ando, M.D., Shotaro Higuchi, M.D., Koichi Ida, M.D., and Tanri Shiozawa, M.D., Ph.D.

1: Department of Obstetrics and Gynecology, Shinshu University School of Medicine, 3-1-1 Asahi, Matsumoto 390-8621, Japan

*** Address correspondence to**: Miyamoto T: Department of Obstetrics and Gynecology, Shinshu University School of Medicine, 3-1-1 Asahi, Matsumoto 390-8621, Japan
Tel: 81-263-37-2719 Fax: 81-263-39-3160 e-mail: tmiya@shinshu-u.ac.jp

Key words:

Lipocalin 2, Reactive Oxygen Species (ROS), ovarian endometriosis, ovarian clear cell carcinoma, oxidative stress, cystine transporter

Abstract

Ovarian clear cell carcinoma (CCC) is arises from ovarian endometriosis. Intra-cystic fluid contains abundant amounts of free iron, which causes persistent oxidative stress, a factor that has been suggested to induce malignant transformation. However, the mechanisms linking oxidative stress and carcinogenesis in CCC currently remain unclear. Lipocalin 2 (LCN2), a multi-functional secretory protein, functions as an iron transporter as well as an antioxidant. Therefore, we herein examined the roles of LCN2 in the regulation of intracellular iron concentrations, oxidative stress, DNA damage, and anti-oxidative functions using LCN2-overexpressing (ES2), and LCN2-silenced (RMG-1) CCC cell lines. The results of calcein staining indicated that the up-regulated expression of LCN2 correlated with increases intracellular iron concentrations. However, a DCFH-DA assay and 8OHdG staining revealed that LCN2 reduced intracellular levels of reactive oxygen species (ROS) and DNA damage. Furthermore, the expression of LCN2 suppressed hydrogen peroxide-induced apoptosis and prolonged cell survival, suggesting an anti-oxidative role for LCN2. The expression of mRNA and protein for various oxidative stress-catalyzing enzymes, such as heme oxygenase (HO), super oxide dismutase (SOD), and glutathione peroxidase, was not affected by LCN2, whereas the intracellular concentration of the potent antioxidant, glutathione (GSH), was increased by LCN2. Furthermore, the expression of xCT, a cystine transporter protein, and CD44 variant 8-10 (CD44v), a stem cell marker, was up-regulated by LCN2. Although LCN2 increased intracellular iron concentrations, LCN2-induced GSH may catalyze and override oxidative stress via CD44v and xCT, and subsequently enhance the survival of CCC cells in oxidative stress-rich endometriosis.

Introduction

Lipocalin 2 (LCN2), also known as neutrophil gelatinase-associated lipocalin (NGAL) or 24p3, is a 25-kDa secretory protein that functions as an iron transporter. LCN2 was initially identified in the granules of neutrophils and as a biostatic agent through its ability to chelate iron around bacteria [1]. LCN2 is known to require siderophores, low molecular weight ferric iron chelators, which bind to iron [1]. LCN2 has been shown to import iron into the cytoplasm after interacting with its specific receptor (SLC22A17, megalin) and increases intracellular iron concentrations [2, 3]. LCN2 also exports intracellular iron, thereby depleting its concentrations [2], and recent studies also revealed that it functioned as an antioxidant [4-7]. LCN2 was found to be up-regulated in sterile inflammation, such as that associated with renal and cardiovascular diseases, and is utilized as a novel diagnostic and prognostic biomarker of these diseases [8-10]. Previous studies demonstrated that LCN2 was up-regulated in several cancers, such as breast, colorectal, gastric, and pancreatic carcinoma, and, thus, has been implicated in the poor prognoses of patients with these cancers [11-15]. We have shown that LCN2 was up-regulated in endometrial carcinoma, and the overexpression of LCN2 and SLC22A17 was associated with the poor prognoses of these patients [16, 17].

Intracellular iron is responsible for the generation of reactive oxygen species (ROS) via the Fenton reaction, and persistent oxidative stress has been shown to induce carcinogenesis [18]. For example, hemochromatosis has been associated with hepatocellular carcinoma [19], and endometriotic cysts have been identified as an origin of CCC [20]. Endometriotic fluid includes high concentrations of free iron, which causes persistent oxidative stress [21]. One of important factors for the development of ovarian carcinoma in endometriotic cyst is DNA damage induced by persistent

oxidative stress [21]. Therefore, we hypothesized that LCN2 was involved in the development of ovarian carcinoma arising from endometriosis by regulating intracellular iron concentrations and oxidative stress. In the present study, we investigated the functions of LCN2 and its mechanisms in CCC cells.

Materials and methods

Cell lines and culture conditions

The CCC cell lines RMG1 and OVISE were purchased from Japanese Collection of Research Bioresources Cell Bank (Osaka, Japan), and ES2, TOV21G were purchased from the ATCC (Manassas, VA). RMG1 cells were cultured in F12 medium (Life Technologies, Carlsbad, CA) supplemented with 10% inactivated fetal bovine serum (FBS) (Life Technologies). OVISE cells were cultured in RPMI 1640 medium (Sigma-Aldrich) with 10% FBS. ES2 cells were cultured in McCoy's 5A (Life Technologies) with 10% FBS. TOV21G cells were cultured in Dulbecco's modified Eagle's medium (Sigma-Aldrich, St. Louis, MO) with 10% FBS. Cells were incubated at 37℃ under 5% CO_2 in air. Recombinant LCN2 (rLCN2) was purchased form Gene Tex (San Antonio, TX). The mean plasma concentration of LCN2 was previously reported to be 72 ng/ml (40-109 ng/ml) in healthy adults [22], and increased 10-fold with acute inflammation [22]. Accordingly, we used rLCN2 concentrations of 200~1000 ng/ml in our experiments.

Establishment of LCN2-overexpressing ES2 and TOV21G cells

The pLenti-L6H plasmid overexpressing NGAL and pLenti-L6H were kindly provided by Dr. Sushovan Guha (The University of Texas MD Anderson Cancer Center, Houston,

Texas, USA). These were transfected into Lenti-293T cells using the Lenti-X HTX Packaging System (Clontech Laboratories, Inc., CA), and lentiviral particles were obtained. ES2 and TOV21G cells were infected with lentiviral particles, and blasticidin was used to select cells. The LCN2-overexpressing cells obtained were named ES2-LCN2 and TOV21G-LCN2, and ES2-mock and TOV21G-mock cells were used as control cells.

Establishment of LCN2-silenced RMG1 and OVISE cells

According to a previous study, LCN2-silenced RMG1 cells (RMG1-shRNA) were established by the transfection of a pGFP-V-RS vector (OriGene Technologies, Rockville, MD) stably producing LCN2-specific short hairpin RNA (shRNA) [23]. The expression of LCN2 in OVISE cells were down-regulated by the transfection of a LCN2 small interfering RNA (siRNA) (OVISE-siRNA) (Life Technologies). Control-RMG1 (RMG1-cont) and OVISE (OVISE-cont) cells were also established by transfection of the same vector producing non-effective scrambled shRNA and siRNA. Real-time RT-PCR revealed that the expression of LCN2 in RMG1-shRNA cells was 97.7% less than that in RMG1-cont cells, and the expression of LCN2 in OVISE–siRNA cells was 70.3% less than that in OVISE-cont cells. Since these vectors included green fluorescent protein (GFP), these cells could not be used in calcein, 2',7'-dichlorofluorescin diacetate (DCFH-DA), or Annexin-V staining.

Reverse transcriptase polymerase chain reaction (RT-PCR) and real-time quantitative PCR

Based on a previous study [23], total RNA was extracted using a TRIzol reagent (Life Technologies) according to the manufacturer's instructions, and reverse-transcribed to cDNA for PCR using the PrimeScript® RT-PCR Kit (Takara Bio, Shiga, Japan). Real-time quantitative PCR was performed using LightCycler® 480 DNA SYBR Green I Master (Roche Diagnostics GmbH, Mannheim, Germany) in LightCycler® 480 system II (Roche Diagnostics GmbH) according to the manufacturer's instructions. The expression of mRNA was quantified using β-actin as an internal control gene. Primer sets are summarized in Suppl. Table 1 [16, 24, 25]. Many of primers were designed using "PrimerBank" (http://pga.mgh.harvard.edu/primerbank/). Each real-time quantitative PCR experiment was independently repeated 3 times with 5 replicates.

ELISA

LCN2 levels of cell culture supernatants were quantified with a solid phase sandwich ELISA using the Human Lipocalin-2/NGAL Immunoassay kit (R&D Systems, Minneapolis, MN) according to the manufacturer's instructions and a previous study [26]. A total of 150000 cells/well were plated onto 24-well plates. After 24 hours, the supernatants were collected and particulates removed by centrifugation. LCN2 levels were then measured. A450 nm was measured by a microplate reader, SYNERGY HT (BioTek, Winooski, VT), and A540 nm was subtracted from readings at A450nm. Each result was obtained from 3 independent experiments with 8 replicates.

Calcein staining

As described previously [2], ES2 cells were stained with 0.75μM calcein-AM (Life Technologies) for 3 minutes at room temperature and observed using a FLoid Cell

Imaging Station fluorescence microscope (Life Technologies). ES2 cells were stained with 0.75μM calcein-AM for 5 minutes, and quantification of the mean intensity of calcein fluorescence in 1×10^5cells was measured by SYNERGY HT.

Western blotting

Proteins extracted from cultured cells were subjected to a Western blot analysis, as described previously [16], using antibodies against CD44 v9 (rat monoclonal; COSMO BIO CO., LTD., Tokyo, Japan), xCT (rabbit monoclonal; Abcam, Cambridge, UK) and β-actin (mouse monoclonal; BioMakor, Rehovot, Israel) as the primary antibody. The membranes were blotted with the primary antibody at 4°C overnight, and then incubated with a peroxidase-conjugated secondary antibody. Bound antibodies were visualized using the ECL Western blot detection reagent (Amersham, Piscataway, NJ).

Immunofluorescence staining

Immunofluorescent staining was performed as described previously [27]. We used mouse monoclonal anti 8-hydroxyguanosine (working concentration 0.65μg/ml, Abcam) and Alexa Fluor® 488 rabbit anti-mouse IgG antibodies (Life Technologies), or rat-monoclonal anti CD44 v9 (working concentration; 3μg/ml) and Alexa Fluor® 594 goat anti-rat IgG antibodies (Life Technologies). Nuclear counterstaining was performed using DAPI-Fluoromount-G (COSMO BIO CO., LTD.). All specimens were observed using a FLoid Cell Imaging Station fluorescence microscope.

WST-1 assay

Cell proliferation/viability was assessed using the WST-1 reagent (Roche Diagnostics

GmbH) according to the manufacturer's instructions and a previous study [23]. Briefly, cells were seeded on 96-well plates. After culturing the cells under various conditions, the WST-1 reagent was added to the medium. After 2.5 h, A450 wavelength light was measured using SYNERGY HT. Each result was obtained from 3 independent experiments with 8 replicates. The absorbance of WST-1 reagent was reported to correlate with the number of viable cells [28].

Cytotoxicity assay

A total of 2000 cells/well were plated on 96-well plates. After 24 hours, the cells were exposed to cytotoxic agents at various concentrations. Hydrogen peroxide (H_2O_2) (Wako, Osaka, Japan) was added to the culture medium for 10 minutes. The medium was then replaced with fresh medium, and cell viability was measured after 48 hours. Iron (III) chloride (WAKO) was added to the culture medium, and cell viability was measured after 48 hours. The anticancer drugs, cisplatin (CDDP) (Sigma-Aldrich) and paclitaxel (PTX) (Wako) were diluted with dimethylformamide (DMFA) and added to the culture medium, and cell viability was measured after 72 hours. Each result was obtained from 3 independent experiments with 8 replicates.

Measurement of ROS

DCFH-DA (non-fluorescent) is rapidly converted to dichlorofluorescin (DCF) (green fluorescent) by ROS in the cytosol. ES2 cells were exposed to 500μM H_2O_2, and incubated with 10μM DCFH-DA (Sigma-Aldrich) for 15 min at 37°C.They were subjected to FLoid Cell Imaging Station fluorescence microscope, and SYNERGY HT in order to quantify of the mean intensity of DCF fluorescence in 5000 cells [25].

Nuclei were stained with Hoechst 33342 (WAKO) for observation by fluorescence microscopy.

GSH Assay

Intracellular levels of GSH (γ-L-glutamyl-L-cysteinyl-glycine) were determined with the GSH-Glo Glutathione Assay kit (Promega). Cell suspensions (8000 cells) were transfered to 1.5 ml microtubes for this assay, which was based on the conversion of a luciferin derivative to luciferin by glutathione S-transferase in the presence of GSH [25]. The signals generated in a coupled reaction with firefly luciferase were proportional to the amount of GSH in the samples. The results obtained were normalized using the GSH standard solution provided with this kit. Each result was obtained from 3 independent experiments with 10 replicates.

Apoptosis assay

Flow cytometry was performed to detect apoptotic cells using the Annexin-V-FLUOS Staining Kit (Roche Applied Science) 24 hours after being treated with 20μM H_2O_2. They were subjected to BD FACScanto II Flow cytometer (BD Biosciences, Tokyo, Japan).

Statistical analysis

Statistical analyses were conducted with Scheffe's test or the Mann-Whitney U test using the SPSS Statistics system (SPSS Inc., Chicago, IL).

Results

215 ***The expression of LCN2 in ovarian carcinoma cell lines***

216 The expression of LCN2 was observed in four ovarian carcinoma cell lines, RMG1,
217 OVISE, ES2, and TOV21G, and the elevated expression of LCN2 at the mRNA and
218 protein levels was confirmed in RMG1 and OVISE cells by RT-PCR (Fig. 1A) and
219 ELISA (Data not shown). The expression of LCN2 in ES2-mock, ES2-LCN2,
220 TOV21G-mock, TOV21G-LCN2, RMG1-cont, RMG1-shRNA, OVISE-cont, and
221 OVISE-siRNA cells was confirmed by RT-PCR (Fig. 1B). LCN2 concentrations in cell
222 culture supernatants were examined by ELISA in ES2-mock (< 0.156 ng/ml,
223 undetectable level), ES2-LCN2 (13.383 ng/ml), TOV21G-mock (< 0.156 ng/ml,
224 undetectable level), TOV21G-LCN2 (0.248ng/ml), RMG1-cont (10.485 ng/ml),
225 RMG1-shRNA (0.216 ng/ml), OVISE-cont (3.92 ng/ml), and OVISE-siRNA (2.21
226 ng/ml) (Figs. 1C). No significant differences were observed in proliferation between
227 ES2-mock and ES2-LCN2, TOV21G-mock and TOV21G-LCN2, RMG1-cont and
228 RMG1-shRNA, and OVISE-cont and OVISE-siRNA cells (Fig. 1D).
229
230 ***LCN2 increased intracellular iron levels***
231 Calcein staining was performed to determine whether LCN2 increased intracellular iron
232 concentrations. Theoretically, nonfluorescent calcein-AM quickly reaches the
233 cytoplasm and is immediately converted to fluorescent calcein. However, iron-bound
234 calcein loses its fluorescence. Therefore, if intracellular iron concentrations are high,
235 calcein fluorescence will be decreased. The results obtained indicated that calcein
236 fluorescence was weaker in ES2-LCN2 cells (Fig. 2A) than in control cells.
237 Furthermore, the same results were obtained when rLCN2 was added to ES2-mock cells
238 (Fig. 2A). The mean intensity of calcein fluorescence was decreased by 82% and 69%,

239 respectively (Fig. 2B), indicating that LCN2 increased intracellular iron concentrations.
240 Intracellular iron concentration is known to affect the expression of iron-responsive
241 genes, such as ferritin (up-regulated) and transferrin receptor 1 (TfR1) (down-regulated)
242 [29]. Therefore, the mRNA levels of these genes were confirmed by real-time RT-PCR.
243 As expected, the expression of ferritin were increased and that of TfR1 were decreased
244 in ES2-LCN2 and ES2-mock treated with rLCN2 compared with that in ES2-mock cells
245 (Fig. 2C).
246
247 ***LCN2 reduced iron-mediated ROS and oxidative stress***
248 Since intracellular iron concentrations were augmented by LCN2, the role of LCN2 in
249 the production of ROS was examined. DCFH-DA is a ROS-sensitive fluorescent probe;
250 when ROS levels are elevated, its green fluorescence is increased. In these experiments,
251 hydrogen peroxide (H_2O_2) was added as a source of oxidative stress, and the subsequent
252 production of intracellular ROS was measured by DCFH-DA staining. We expected
253 LCN2 to induce ROS and oxidative stress by increasing intracellular iron concentrations.
254 However, green fluorescence was decreased in ES2-LCN2 cells and rLCN2-added
255 ES2-mock (ES2-mock with rLCN2) cells (Fig. 3A). The addition of H_2O_2 to ES2-mock
256 cells increased the mean fluorescence by 3.33-fold that of the untreated control cells.
257 However, its intensity only increased by 1.33-fold and 1.06-fold in ES2-LCN2 and
258 ES2-mock with rLCN2 cells, respectively (Fig. 3B). These results indicated that LCN2
259 reduced ROS.
260 8-hydroxy-2'-deoxyguanosine (8OHdG) is an oxidative DNA damage marker.
261 8OHdG immunofluorescence was examined in ES2 cells after the treatment with H_2O_2
262 in order to investigate the relationship between LCN2 and oxidative DNA damage *in*

263 *vitro*. 8OHdG fluorescence was weaker in ES2-LCN2 cells and ES2-mock with rLCN2
264 cells than in control cells (Fig. 3C). The cell viability of ES2-LCN2 cells was higher
265 than that of control cells after the treatment with H_2O_2 and ferric iron (Fig. 3D). The
266 immunohistochemical expression of 8OHdG in ovarian carcinoma tissues and
267 endometriotic cysts was then examined. The expression of 8OHdG was low in cases of
268 ovarian carcinoma and endometriosis that strongly expressed LCN2 (Suppl. Figs 1A, C,
269 E). In contrast, the expression of 8OHdG was high in cases of ovarian carcinoma and
270 endometriosis that weakly expressed LCN2 (Suppl. Figs. 1B, D, F). In addition, an
271 inverse correlation between LCN2 expression and 8OHdG expression was observed in
272 20 cases of CCC (R2 =0.494, P=0.001) (Suppl. Fig. 1C). These results suggested that
273 LCN2 reduced DNA damage caused by oxidative stress.
274
275 ***LCN2 inhibited apoptosis induced by oxidative stress and enhanced cell survival.***
276 A flow cytometric analysis was performed using immunofluorescence for annexin-V
277 and propidium iodide (PI) in order to determine whether LCN2 inhibited oxidative
278 stress-induced apoptosis. The results obtained indicated that the forced expression of
279 LCN2 decreased apoptosis after the H_2O_2 treatment in ES2 cells (Fig. 4). Moreover, cell
280 viability was examined using the WST-1 assay in cells treated with cisplatin and
281 paclitaxel to examine whether LCN2 enhanced chemoresistance. The cell viability of
282 ES2-LCN2 and TOV21G-LCN2 cells was higher than that of control cells after the
283 treatment with cisplatin and paclitaxel (Figs. 5A, B). These results indicated that LCN2
284 inhibited apoptosis and enhanced chemoresistance.
285
286 ***LCN2 increased intracellular GSH levels and enhanced the expression of the CD44***

variant and xCT.

Since LCN2 was expected to enhance antioxidant functions, the mRNA levels of toxic ROS-catalyzing enzymes, including heme oxygenase (HO), superoxide dismutase (SOD), catalase, glutathione peroxidase (GPx), and peroxiredoxin (PRDX) were examined using real-time quantitative PCR in ES2-mock and ES2-LCN2 cells. However, the forced expression of LCN2 did not increase the expression of these antioxidant enzymes (Suppl. Fig. 2A). Furthermore, no significant difference was observed in the protein expression of HO-1, HO-2, SOD1, and SOD2 (data not shown). However, the concentration of another important antioxidant, glutathione (GSH), was significantly higher in ES2-LCN2 and TOV21G-LCN2 cells than that in control cells (Fig. 5C), suggesting that LCN2 increased intracellular GSH concentrations.

The role of LCN2 in the cystine transport system was examined because GSH is synthesized from cysteine, a precursor of GSH. CD44 variant 8-10 (CD44v) has been shown to interact with and stabilize xCT, a cystine-glutamate exchange transporter, and promotes the uptake of cystine for intracellular GSH synthesis [21]. The expression of CD44v mRNA was not significantly different, irrespective of the LCN2 status (Suppl. Fig 2B); however, CD44v protein expression was increased by the addition of rLCN2 (500 ng/ml) and forced expression of LCN2 as observed by CD44v immunofluorescence (Fig. 5D) and western blotting (Fig. 5E). Likewise, xCT protein expression was increased by the addition of rLCN2 (500 ng/ml) and forced expression of LCN2 (Fig. 5F). However, the expression of xCT mRNA was not affected by LCN2 (Suppl. Fig 2C). In contrast, the cell viability of RMG1-shRNA cells was lower than that of control cells after the treatment with cisplatin and paclitaxel (Fig. 6A). The cell viability of OVISE-siRNA cells was also lower than that of control cells after the

311 treatment with paclitaxel (Suppl. Fig. 3A). The intracellular GSH concentration was
312 significantly lower in RMG1-shRNA (Fig. 6B) and OVISE-siRNA cells (Suppl. Fig.
313 3B) than that in control cells. Although the CD44v and xCT mRNA expression was not
314 significantly difference between RMG1-cont and RMG1-siRNA (Suppl. Figs 2 B, C),
315 the CD44v and xCT protein expression was decreased by the reduced expression of
316 LCN2, as observed by immunofluorescence (Fig. 6C) and western blotting (Fig. 6D).
317 To investigate whether LCN2 affect the stabilization of CD44v and xCT, we measured
318 these protein levels treated with CHX to inhibit protein synthesis. Western blotting
319 revealed that the degradation of CD44v and xCT was delayed in ES2-LCN2 cells
320 compared with that in ES2-mock cells (Supplementary figs. 4). The delayed degradation
321 of xCT was observed also in TOV21G-LCN2 cells. These results suggested that LCN2
322 enhanced the expression of the CD44v and xCT protein through the stabilizing CD44v
323 and xCT, and increased intracellular GSH levels, resulting in a decrease in oxidative
324 stress and prolonged cell survival.
325

326 **Discussion**

327 Ovarian endometriosis (OEM) has been identified as an origin of CCC and
328 endometrioid carcinoma [20]. Since its fluid includes high concentrations of free iron,
329 which generates persistent oxidative stress, DNA damage induced by persistent
330 oxidative stress is considered to be involved in the development of ovarian carcinoma
331 arising from OEM [21]. Therefore, we herein focused on LCN2, an iron transporter,
332 because it is known to bind to iron, import it into the cytoplasm, and increase its
333 intracellular concentrations [2]. The results obtained by calcein staining demonstrated
334 that LCN2 increased intracellular iron concentrations in ES2 cells. Mandai et al.

reported that free iron and hypoxia in OEM induced ROS, oxidative stress, and disordered gene repair, which led to the accumulation of DNA mutations and cancer development [30]. We hypothesized that LCN2 was involved in the development of CCC by increasing intracellular iron concentrations, ROS, and oxidative stress.

The intake of iron, a source of oxidative stress, is essential for maintaining the normal functions of human cells [31]. However, excess iron uptake is not advantageous because toxic iron-mediated oxidative stress is detrimental to cells [32]. For example, the epithelial lining of endometriotic cysts from which CCC arises, often degenerated and exfoliated, possibly due to iron-induced oxidative stress in the intra-cystic fluid. In this context, we first presumed that the LCN2-mediated augmentation of iron resulted in increases in ROS and oxidative stress in CCC cells. However, the results obtained by DCFH-DA staining and 8OHdG immunofluorescence revealed that LCN2 decreased ROS and oxidative stress. LCN2 was previously shown to be induced by oxidative stress [33], and protects cells from oxidative stress [4-7]. It is also induced under several harmful conditions, such as endoplasmic reticulum (ER) stress and thermal stress, and protects cells against these stresses [34-36]. These findings indicate that LCN2 is a stress-responsive molecule that protects against various stresses. Collectively, stress-induced LCN2 overrides the negative effects of uptaking iron, and scavenges ROS in order to ameliorate oxidative stress.

Regarding the LCN2-mediated, anti-oxidant function of ES2 cells, we first focused on the involvement of antioxidative enzymes. Bahmani et al. previously reported that LCN2 induced the expression of HO-1, SOD-1 and SOD-2 [5]. Halabian et al. showed that LCN2 induced the expression of HO-1, SOD-1, and metallothionein 1,

359 and also increased the activities of HO-1 and SOD [7]. However, no significant
360 difference was observed in these antioxidative enzymes between ES2-mock and
361 ES2-LCN2 cells. The present study demonstrated that LCN2 induced the up-regulation
362 of another important antioxidant, GSH. GSH maintains enzyme and protein thiols in
363 their reduced state, and scavenges free radicals and other reactive oxygen species [37].
364 Tanner et al. reported that GSH levels in ovarian carcinoma tissue specimens obtained
365 from surgery were higher in the advanced stage, and the survival of patients with high
366 GSH levels in ovarian carcinoma tissue specimens was significantly shorter [38]. We
367 considered LCN2-induced GSH to have reduced ROS and oxidative stress and played
368 an important role in tolerance against oxidative stress and chemoresistance enhanced by
369 LCN2.

370 CD44 is a stem cell marker that has various variant isoforms [39]. The full-length
371 CD44 gene has 20 exons and 19 introns, and genomic exon numbers 6-15 are variable
372 exons that are numbered v1-10 [39]. CD44 variant 8-10 (CD44v), which has v8, v9, and
373 v10 and is a specific marker for gastric cancer stem cells [24], was shown to increase
374 intracellular GSH levels in cancer stem cells by stabilizing xCT and play a central role
375 in resistance to cancer therapy [25]. System xc^- is a cystine-glutamate transporter
376 composed of xCT, a light-chain subunit, and CD98hc, a heavy-chain subunit [40]. The
377 expression of xCT on the cell surface is essential for the uptake of cystine [40]. Cystine
378 is important for the intracellular synthesis of GSH because it is rapidly converted to
379 cysteine, and which is utilized for GSH synthesis [37] and has been identified as a rate
380 limiting factor in GSH synthesis [41]. Our results suggested that LCN2 induced the
381 expression of the CD44v and xCT proteins. Since no significant difference was
382 observed in the expression of CD44v and xCT mRNA, these proteins may be involved

in post translational regulation. We speculated that LCN2 interacted with CD44v and xCT on the cell surface and enhanced their stabilities. Since the direct interaction between LCN2 and xCT/CD44v had not been demonstrated (data not shown), we consider that LCN2 might interact to xCT/CD44v through other protein, such as MMP-9. MMP-9 is known to interact to both LCN2 and CD44 [42, 43]. Recently, Sakakura reported that xCT protected neutrophils from apoptosis induced by ROS which was produced to kill microorganism [44]. LCN2 may contribute to enhance the expression of xCT in neutrophils, because neutrophils are known to have much LCN2 and release them by infection. To the best of our knowledge, this is the first study to show that LCN2 mediated GSH via CD44v and xCT.

On the other hand, Bao et al. reported that LCN2 formed a complex with epigallocatechin-3-gallate and iron, and inhibited the chemical reactivity of iron, such as the Fenton reaction [45]. This finding suggested that extracellular LCN2 secreted by cells chelated iron, inhibited the Fenton reaction, and reduced the production of ROS. Although a previous study implicated high concentrations of free iron in endometriotic fluid in persistent oxidative stress and the subsequent development of cancer [21], excess oxidative stress is known to be lethal for cells [32]. In the early stage of OME formation, the oxidative stress-rich environment is likely to kill the lining cells of OME because most inner lining cells of surgically obtained OEM are exfoliated and lost. On the other hand, the accumulation of oxidative stress-induced DNA damage may cause the malignant transformation of OEM lining cells, if the OEM lining cell survives under such toxic conditions. We hypothesized that OEM lining cells may express LCN2 in order to reduce oxidative stress by chelating iron and increasing intracellular GSH levels as well as the expressions of CD44v and xCT, leading to cell survival under such

407 severe oxidative circumstances. Therefore, we considered CCC to arise from surviving
408 OEM lining cells, and LCN2 to promote the malignant potential of CCC. Further
409 studies are needed to confirm this hypothesis.
410 Lee et al. recently reported that an injection of an LCN2 antibody into nude mice
411 markedly reduced the growth of RL95-2, an endometrial cancer cell line that expresses
412 abundant amount of LCN2 [46]. This finding indicates that LCN2 has the potential to be
413 a valuable therapeutic target.
414 In conclusion, the present study demonstrated that LCN2 increased intracellular
415 iron, but decreased ROS and oxidative stress, suggesting its function as an antioxidant.
416 Its effects were promoted by an increase in the expression of GSH mediated by the
417 CD44 variant and xCT proteins. LCN2 eventually inhibits apoptosis and prolongs cell
418 survival under various stress conditions, including oxidative stress and chemotherapy,
419 thereby providing advantageous characteristics to cancer cells for the development of
420 stress-rich endometriotic cysts. This function indicates that LCN2 is a good therapeutic
421 target, and further studies are needed for clinical applications.
422

423 **Acknowledgment**

424 This work was supported by JSPS KAKENHI Grant Number 25861484.
425

426 **Declaration of Interest**

427 The authors declare that there are no conflicts of interest.
428
429

References

[1] Flo TH, Smith KD, Sato S, Rodriquez DJ, Holmes MA, Strong RK, Akira S, Aderem A. Lipocalin 2 mediates an innate immune response to bacterial infection by sequestrating iron. Nature 2004; 432: 917-921.

[2] Devireddy LR, Gazin C, Zhu X, Green MR. A cell-surface receptor for lipocalin 24p3 selectively mediates apoptosis and iron uptake. Cell 2005; 123: 1293-1305.

[3] Hvidberg V, Jacobsen C, Strong RK, Cowland JB, Moestrup SK, Borregaard N. The endocytic receptor megalin binds the iron transporting neutrophil-gelatinase-associated lipocalin with high affinity and mediates its cellular uptake. FEBS Lett. 2005; 579: 773-777.

[4] Roudkenar MH, Halabian R, Ghasemipour Z, Roushandeh AM, Rouhbakhsh M, Nekogoftar M, Kuwahara Y, Fukumoto M, Shokrgozar MA. Neutrophil gelatinase-associated lipocalin acts as a protective factor against H_2O_2 toxicity. Arch Med Res. 2008; 39: 560-566.

[5] Bahmani P, Halabian R, Rouhbakhsh M, Roushandeh AM, Masroori N, Ebrahimi M, Samadikuchaksaraei A, Shokrgozar MR, Roudkenar MH. Neutrophil gelatinase-associated lipocalin induces the expression of heme oxygenase-1 and superoxide dismutase 1, 2. Cell Stress Chaperones 2010; 15: 395-403.

[6] Roudkenar MH, Halabian R, Bahmani P, Roushandeh AM, Kuwahara Y, Fukumoto M. Neutrophil gelatinase-associated lipocalin: A new antioxidant that exerts its cytoprotective effect independent on Heme Oxygenase-1. Free Radic Res. 2011; 45: 810-819.

[7] Halabian R, Tehrani HA, Jahanian-Najafabadi A, Roudkenar MH. Lipocalin-2-mediated upregulation of various antioxidants and growth factors

protects bone marrow-derived mesenchymal stem cells against unfavorable microenvironments. Cell Stress Chaperones 2013; 18: 785-800.

[8] Catalan V, Gomez-Ambrosi J, Rodriguez A, Ramirez B, Silva C, Rotellar F, Gil MJ, Cienfuegos JA, Salvador J, Fruhbeck G. Increased adipose tissue expression of lipocalin-2 in obesity is related to inflammation and matrix metalloproteinase-2 and metalloproteinase-9 activities in humans. J Mol Med. 2009; 87: 803-813.

[9] Sahinarsian A, Kocaman SA, Bas D, Akyel A, Ercin U, Zengin O, Timurkaynak T. Plasma neutrophil gelatinase-associated lipocalin levels in acute myocardial infarction and stable coronary artery disease. Coron Artery Dis. 2011; 22: 333-338.

[10] Viau A , El Karoui K, Laouari D, Burtin M, Nguyen C, Mori K, Pillebout E, Berger T, Mak TW, Knebelmann B, Friedlander G, Barasch J, Terzi F. Lipocalin 2 is essential for chronic kidney disease progression in mice and humans. J Clin Invest. 2010; 120: 4065-4076.

[11] Bauer M, Eickhoff JC, Gould MN, Mundhenke C, Maass N, Friedl A. Neutrophil gelatinase-associated lipocalin (NGAL) is a predictor of poor prognosis in human primary breast cancer. Breast Cancer Res Treat 2008; 108: 389-397

[12] Leng X, Ding T, Lin H, Wang Y, Hu L, Hu J, Feig B, Zhang W, Pusztai L, Symmans WF, Wu Y, Arlinghaus RB. Inhibition of lipocalin 2 impairs breast tumorigenesis and metastasis. Cancer Res 2009; 69: 8579-8584

[13] Barresi V, Reggiani-Bonetti L, Di Gregorio C, Vitarelli E, Ponz De Leon M, Barresi G. Neutrophil gelatinase-associated lipocalin (NGAL) and matrix metalloproteinase-9 (MMP-9) prognostic value in stage I colorectal carcinoma. Pathol Res Pract. 2011; 207: 479-486.

[14] Wang HJ, He XJ, Ma YY, Jiang XT, Xia YJ, Ye ZY, Zhao ZS, Tao HQ. Expressions

478 of neutrophil gelatinase-associated lipocalin in gastric cancer: a potential biomarker
479 for prognosis and an ancillary diagnostic test. Anat Rec. 2010; 293:1855-1863
480 [15] Tong Z, Kunnumakkara AB, Wang H, Matsuo Y, Diagaradjane P, Harikumar
481 KB, Ramachandran V, Sung B, Chakraborty A, Bresalier RS, Logsdon C, Aggarwal
482 BB, Krishnan S, Guha S. Neutrophil gelatinase-associated lipocalin: a novel
483 suppressor of invasion and angiogenesis in pancreatic cancer. Cancer Res. 2008;
484 68: 6100-6108.
485 [16] Miyamoto T, Kashima H, Suzuki A, Kikuchi N, Konishi I, Seki N, Shiozawa T.
486 Laser-captured microdissection-microarray analysis of the genes involved in
487 endometrial carcinogenesis: stepwise up-regulation of lipocalin2 expression in
488 normal and neoplastic endometria and its functional relevance. Hum Pathol. 2011;
489 42: 1265-1274.
490 [17] Miyamoto T, Asaka R, Suzuki A, Takatsu A, Kashima H, Shiozawa T.
491 Immunohistochemical detection of a specific receptor for lipocalin2 (solute carrier
492 family 22 member 17, SLC22A17) and its prognostic significance in endometrial
493 carcinoma. Exp Mol Pathol. 2011; 91: 563–568
494 [18] Toyokuni S. Role of iron in carcinogenesis: Cancer as a ferrotoxic disease. Cancer
495 Sci. 2009; 100: 9-16.
496 [19] Bradbear RA, Bain C, Siskind V, Schofield FD, Webb S, Axelsen EM, Halliday
497 JW, Bassett ML, Powell LW. Cohort study of internal malignancy in genetic
498 hemochromatosis and other chronic nonalcoholic liver diseases. J Natl Cancer Inst.
499 1985; 75: 81– 4.
500 [20] Kobayashi H, Sumimoto K, Moniwa N, Imai M, Takakura K, Kuromaki T, Morioka

E, Arisawa K, Terao T. Risk of developing ovarian cancer among women with ovarian endometrioma: a cohort study in Shizuoka, Japan. Int J Gynecol Cancer 2007; 17: 37–43.

[21] Yamaguchi K, Mandai M, Toyokuni S, Hamanishi J, Higuchi T, Takakura K, Fujii S. Contents of endometriotic cysts, especially the high concentration of free iron, are a possible cause of carcinogenesis in the cysts through the iron-induced persistent oxidative stress. Clin Cancer Res. 2008; 14: 32-40.

[22] Axelsson L, Bergenfeldt M, Ohlsson K. Studies of the release and turnover of a human neutrophil lipocalin. Scand J Clin Lab Invest. 1995; 55: 577-588.

[23] Kobara H, Miyamoto T, Suzuki A, Asaka R, Yamada Y, Ishikawa K, Kikuchi N, Ohira S, Shiozawa T. Lipocalin2 enhances the matrix metalloproteinase-9 activity and invasion of extravillous trophoblasts under hypoxia. Placenta 2013; 34: 1036-1043.

[24] Lau WM, Teng E, Chong HS, Lopez KA, Tay AY, Salto-Tellez M, Shabbir A, So JB, Chan SL. CD44v8-10 is a cancer-specific marker for gastric cancer stem cells. Cancer Res. 2014; 74: 2630-2641.

[25] Ishimoto T, Nagano O, Yae T, Tamada M, Motohara T, Oshima H, Oshima M, Ikeda T, Asaba R, Yagi H, Masuko T, Shimizu T, Ishikawa T, Kai K, Takahashi E,Imamura Y, Baba Y, Ohmura M, Suematsu M, Baba H, Saya H. CD44 variant regulates redox atatus in cancer cells by stabilizing the xCT subunit of system xc– and thereby promotes tumor growth. Cancer Cell 2011; 19: 387-400

[26] Cho H, Kim JH. Lipocalin2 expressions correlate significantly with tumor differentiation in epithelial ovarian cancer. J Histochem Cytochem. 2009; 57: 513-521.

525 [27] Kikuchi N, Horiuchi A, Osada R, Imai T, Wang C, Chen X, Konishi I. Nuclear
526 expression of S100A4 is associated with aggressive behavior of epithelial ovarian
527 carcinoma: an important autocrine/paracrine factor in tumor progression. Cancer
528 Sci. 2006; 97: 1061-1069.
529 [28] Ishiyama M, Tominaga H, Shiga M, Sasamoto K, Ohkura Y, Ueno K. A combined
530 assay cell viability and in vitro cytotoxicity with a highly water-soluble tetrazolium
531 salt, neutral red and crystal violet. Bio Pharm Bull. 1996; 11: 1518-20.
532 [29] Brewer CJ, Wood RI, Wood JC. mRNA regulation of iron transporters and ferritin
533 subunits in a mouse model of iron overload. Exp Hematol. 2014; 42: 1059-67.
534 [30] Mandai M, Matsumura N, Baba T, Yamaguchi K, Hamanishi J, Konishi I. Ovarian
535 clear cell carcinoma as a stress-responsive cancer: Influence of the
536 microenvironment on the carcinogenesis and cancer phenotype. Cancer Lett. 2011;
537 310: 129-133.
538 [31] Heath JL, Weiss JM, Lavau CP, Wechsler DS. Iron deprivation in cancer—potential
539 therapeutic implications. Nutrients 2013; 5: 2836-2859.
540 [32] Trachootham D, Alexandre J, Huang P. Targeting cancer cells by ROS-mediated
541 mechanisms: a radical therapeutic approach? Nat Rev Drug Discov. 2009; 8: 579–
542 591.
543 [33] Roudkenar MH, Kuwahara Y, Baba T, Roushandeh AM, Ebishima S, Abe
544 S, Ohkubo Y, Fukumoto M. Oxidative stress induced lipocalin 2 gene expression:
545 addressing its expression under the harmful conditions. J. Radiat Res. 2007; 48:
546 39-44

547 [34] Mahadevan MR, Rodvold J, Almanza G, Perez AF, Wheeler MC, Zanetti M. ER
548 stress drives Lipocalin 2 upregulation in prostate cancer cells in an
549 NF-κ B-dependent manner. BMC Cancer 2011; 11: 229.
550 [35] Kumandan S, Mahadevan NR, Chiu K, DeLaney A, Zanetti M. Activation of the
551 unfolded protein response bypasses trastuzumab-mediated inhibition of the PI-3K
552 pathway. Cancer Lett. 2013; 329: 236-242
553 [36] Roudkenar MH, Halabian R, Roushandeh AM, Nourani MR, Masroori N, Ebrahimi
554 M, Nikogoftar M, Rouhbakhsh M, Bahmani P, Najafabadi AJ, Shokrgozar MA.
555 Lipocalin2 regulation by thermal stresses: protective role of Lcn2/ NGAL against
556 cold and heat stresses. Exp Cell Res. 2009; 315: 3140-3151.
557 [37] Wu G, Fang YZ, Yang S, Lupton JR, Turner ND. Glutathione metabolism and its
558 implications for health. J Nutr. 2004; 134: 489-492.
559 [38] Tanner B, Hengstler JG, Dietrich B, Henrich M, Steinberg P, Weikel W, Meinert R,
560 Kaina B, Oesch F, Knapstein PG. Glutathione, glutathione S-transferase alpha and
561 pi, and aldehyde dehydrogenase content in relationship to drug resistance in ovarian
562 cancer. Gynecol Oncol. 1997; 65: 54-62.
563 [39] Williams K, Motiani K, Giridhar PV, Kasper S. CD44 integrates signaling in
564 normal stem cell, cancer stem cell and (pre)metastatic niches. Exp Bio Med. 2013;
565 238: 324-338.
566 [40] Fotiadis D, Kanai Y, Palacín M. The SLC3 and SLC7 families of amino acid
567 transporters. Mol Aspects Med. 2013; 34: 139-158.
568 [41] Bannai S, Tateishi N. Role of membrane transport in metabolism and function of
569 glutathione in mammals. J Membr Biol. 1986; 89: 1-8.
570 [42] Peng ST, Su CH, Kuo CC, Shaw CF, Wang HS. CD44 crosslinking-mediated

matrix metalloproteinase-9 relocation in breast tumor cells leads to enhanced metastasis. Int J Oncol. 2007; 31: 1119-26.

[43] Yan L, Borregaard N, Kjeldsen L, Moses MA. The high molecular weight urinary matrix metalloproteinase (MMP) activity is a complex of gelatinase B/MMP-9 and neutrophil gelatinase-associated lipocalin (NGAL). Modulation of MMP-9 activity by NGAL. J Biol Chem. 2001; 276: 37258-65.

[44] Sakakura Y, Sato H, Shiiya A, Tamba M, Sagara J, Matsuda M, Okamura N, Makino N, Bannai S. Expression and function of cystine/glutamate transporter in neutrophils. J Leukoc Biol. 2007; 81: 974-982.

[45] Bao GH, Xu J, Hu FL, Wan XC, Deng SX, Barasch J. EGCG inhibit chemical reactivity of iron through forming an Ngal-EGCG-iron complex. Biometals 2013; 26: 1041-1050.

[46] Lee YC, Tzeng WF, Chiou TJ, Chu ST. MicroRNA-138 suppresses neutrophil gelatinase-associated lipocalin expression and inhibits tumorigenicity. PLoS One. 2012; 7: e52979.

586 **Figure legends**

587 **Fig.1**

588 **A:** LCN2 mRNA expression in ovarian carcinoma cell lines by RT-PCR. RMG1 and
589 OVISE cells expressed LCN2 mRNA, whereas the others did not. **B:** LCN2 mRNA
590 expression in ES2-mock, ES2-LCN2, TOV21-mock, TOV21G-LCN2, RMG1-cont,
591 RMG1-shRNA, OVISE-cont, and OVISE-siRNA cells by RT-PCR. LCN2 mRNA
592 expression was up-regulated in ES2-LCN2 and TOV21G-LCN2, and suppressed in
593 RMG1-shRNA and OVISE-siRNA. **C:** LCN2 protein levels in supernatants by ELISA
594 in ES2-mock (U: undetectable), ES2-LCN2 (13.383 ng/ml), TOV21G-mock (U),
595 TOV21G-LCN2 (0.248 ng/ml), RMG-cont (10.485 ng/ml), RMG-shRNA (0.216 ng/ml),
596 OVISE-cont (3.92 ng/ml), and OVISE-siRNA (2.21 ng/ml) cells. **D:** Relative cell
597 viability between ES2-mock and ES2-LCN2, TOV21G-mock and TOV21G-LCN2,
598 RMG1-cont and RMG1-shRNA, or OVISE-cont and OVISE-siRNA as determined by
599 the WST-1 assay. No significant difference was noted among these cells.
600 ***: $P<0.001$. Error bars show the standard deviation.
601

602 **Fig.2**

603 **A:** Calcein staining (calcein-AM 0.75μM, 3 minutes) in ES2-mock, ES2-mock with
604 rLCN2 (1000 ng/ml), and ES2-LCN2 cells. Iron concentrations were increased in the
605 latter two cells. **B:** The intensity of calcein fluorescence was measured for 24000 cells
606 by a microplate reader (calcein-AM 0.75μM, 5 minutes) in ES2-mock, ES2-mock with
607 rLCN2 (1000 ng/ml), and ES2-LCN2 cells. The latter two cells showed significantly
608 weaker calcein fluorescence. **C:** The mRNA expression of ferritin and transferrin
609 receptor 1 (TfR1) in ES2-mock and ES2-LCN2 by real-time RT-PCR. The mRNA

610 levels of ferritin were increased and those of TfR1 were decreased in ES2-LCN2 and
611 ES2-mock treated with rLCN2.
612 *:P<0.05, ***: P<0.0001. Error bars show the standard deviation.
613
614 **Fig.3**
615 **A:** DCFH-DA and Hoechst 33342 (blue, nuclei) staining in ES2 cells. DCFH-DA
616 (non-fluorescent) was converted to DCF (green fluorescent) by intracellular ROS. The
617 green fluorescence reflecting the intracellular ROS level was negligible in the cells
618 untreated with H_2O_2 (upper panels). ES2 cells treated with 500μM H_2O_2 for 20 minutes
619 (lower panels). The green fluorescence was detected in ES2-mock cells (lower left), but
620 was negligible in ES2-mock with rLCN2 (500 ng/ml) and ES2-LCN2 cells (lower
621 center and right). **B:** The intensity of DCF fluorescence was measured by a microplate
622 reader. The fluorescence of ES2 cells treated with 500μM H_2O_2 was relative to the
623 fluorescence of untreated ES2 cells. ES2-mock with rLCN2 (500 ng/ml) and ES2-LCN2
624 cells had significantly lower ROS levels than ES2-mock cells. **C:** Immunofluorescence
625 staining for 8OHdG in ES2 cells treated with 0.8μM H_2O_2 for 24 hours. The green
626 fluorescence of 8OHdG was only observed in ES2-mock cells.
627 **D:** Relative cell viability treated with H_2O_2 and with $FeCl_3$ by the WST1 assay. Cell
628 viability was higher in ES2-LCN2 cells than in ES2-mock cells.
629 *: P<0.05, **: P<0.01. Error bars show the standard deviation.
630
631 **Fig. 4**
632 Flow cytometry for Annexin-V and PI in ES2 cells. Early and late apoptotic cells
633 increased from 3.3% to 13.3% and from 8.4% to 16.6% in ES2-mock cells by the

treatment with H_2O_2, respectively. However, no increase was observed in ES2-LCN2 cells.

Fig. 5

A: Ratio of absorbance in ES2 cells treated with cisplatin and paclitaxel by the WST1 assay. The cell viability of ES2-LCN2 cells was higher than that of ES2-mock cells. **B:** Ratio of absorbance in TOV21G cells treated with cisplatin and paclitaxel by the WST1 assay. The cell viability of TOV21G-LCN2 cells was higher than that of TOV21G-mock cells. **C:** Intracellular GSH levels in ES2 (left) and TOV21G cells (right). Intracellular GSH levels were higher in ES2-LCN2 and TOV21G-LCN2 cells than in those of control cells. **D:** Immunofluorescence for CD44v (red) in ES2 cells. The blue color indicated nuclear counterstaining by DAPI. Strong staining for CD44v was detected under LCN2-positive conditions. **E:** CD44v protein expression in ES2 by Western blotting. The numeric values under each graph were the ratios of band densities calculated by a densitometer. The expression of the CD44v protein was significantly increased under LCN2-positive conditions. **F:** xCT protein expression in ES2 by Western blotting. The numeric values under each graph were the ratios of band densities calculated by a densitometer. The expression of the xCT protein was significantly increased under LCN2-positive conditions.The concentration of rLCN2 was 500 ng/ml.*: $P<0.05$, **: $P<0.01$. Error bars show the standard deviation.

Fig. 6

A: Ratio of absorbance in RMG1 cells treated with cisplatin and paclitaxel by the WST1 assay. The cell viability of RMG1-cont cells was higher than that of

RMG1-shRNA cells. **B:** Intracellular GSH levels in RMG1 cells. Intracellular GSH levels were lower in RMG1-shRNA than in that in control cells. **C:** **I**mmunofluorescence for CD44v (red) in RMG1 cells. The blue color indicated nuclear counterstaining by DAPI. Strong staining for CD44v was detected under LCN2-positive conditions. **D:** CD44v and xCT protein expression in RMG1 cells by Western blotting. The numeric values under each graph were the ratios of band densities calculated by a densitometer. The expression of the CD44v and xCT protein was significantly increased under LCN2-positive conditions. The concentration of rLCN2 was 500 ng/ml. *: $P<0.05$, **: $P<0.01$. ***: $P<0.001$. Error bars show the standard deviation."

Figure 1

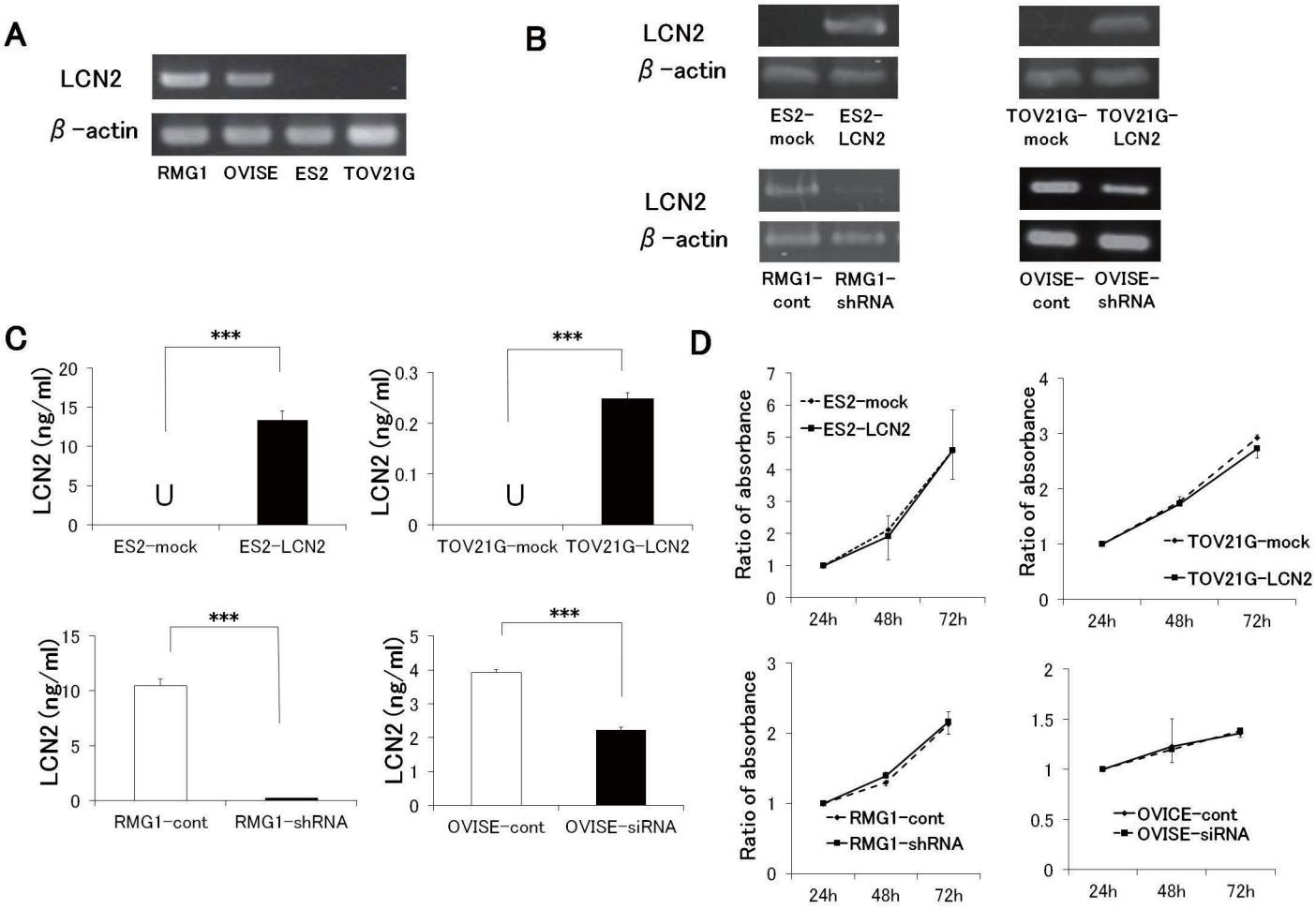
A
LCN2
β -actin
RMG1 OVISE ES2 TOV21G
B
LCN2
β -actin
ES2- mock
ES2- LCN2
TOV21G- mock
TOV21G- LCN2
LCN2
β -actin
RMG1- cont
RMG1- shRNA
OVISE- cont
OVISE- shRNA
C
LCN2 (ng/ml)
***
U
ES2-mock
ES2-LCN2
TOV21G-mock
TOV21G-LCN2
RMG1-cont
RMG1-shRNA
OVISE-cont
OVISE-siRNA
D
Ratio of absorbance
ES2-mock
ES2-LCN2
TOV21G-mock
TOV21G-LCN2
RMG1-cont
RMG1-shRNA
OVICE-cont
OVISE-siRNA
24h
48h
72h

Figure 2

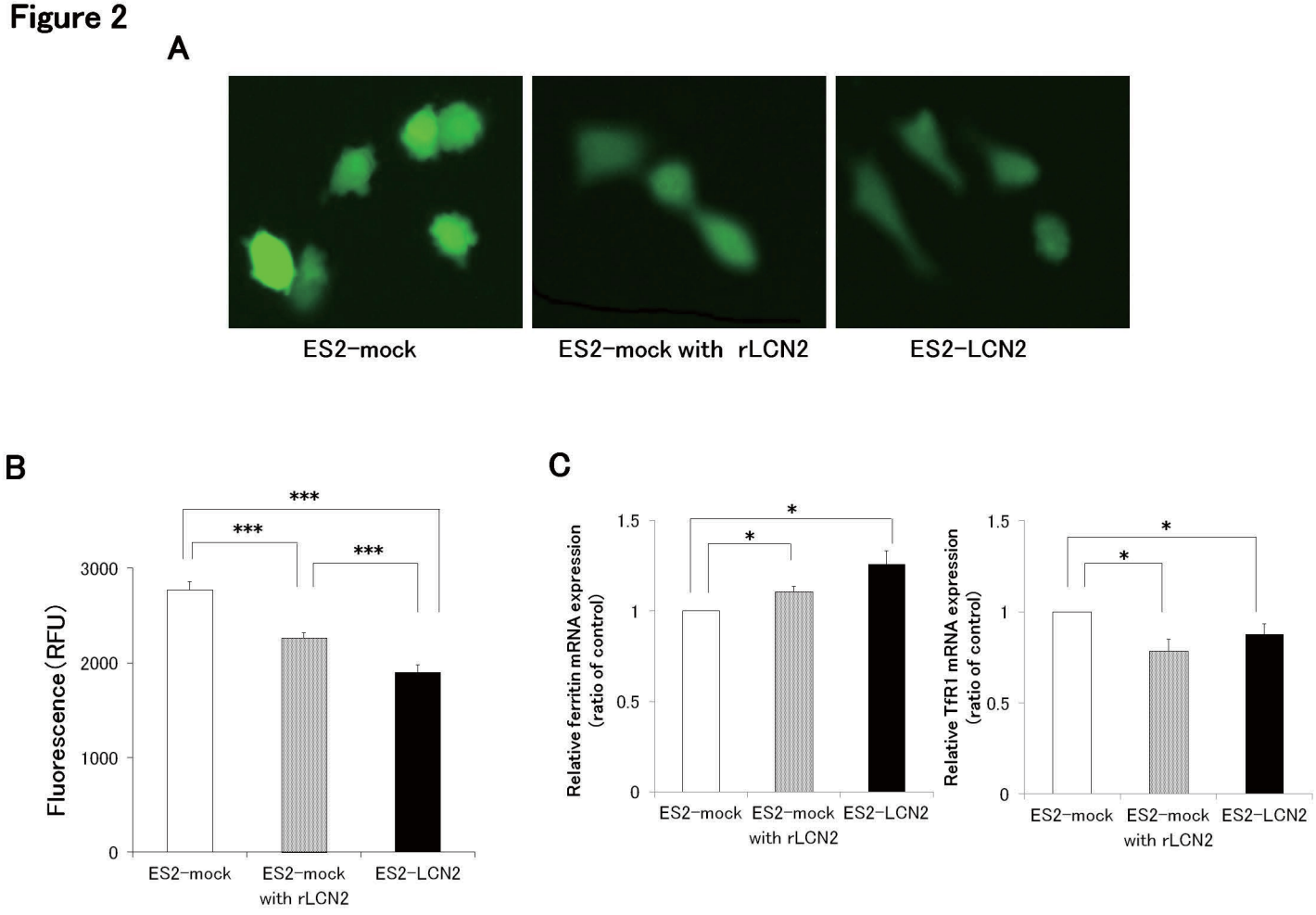
A
ES2-mock
ES2-mock with rLCN2
ES2-LCN2
B
Fluorescence (RFU)
3000
2000
1000
0
***
***
***
ES2-mock
ES2-mock with rLCN2
ES2-LCN2
C
Relative ferritin mRNA expression (ratio of control)
1.5
1
0.5
0
*
*
ES2-mock
ES2-mock with rLCN2
ES2-LCN2
Relative TfR1 mRNA expression (ratio of control)
1.5
1
0.5
0
*
*
ES2-mock
ES2-mock with rLCN2
ES2-LCN2

Figure 3

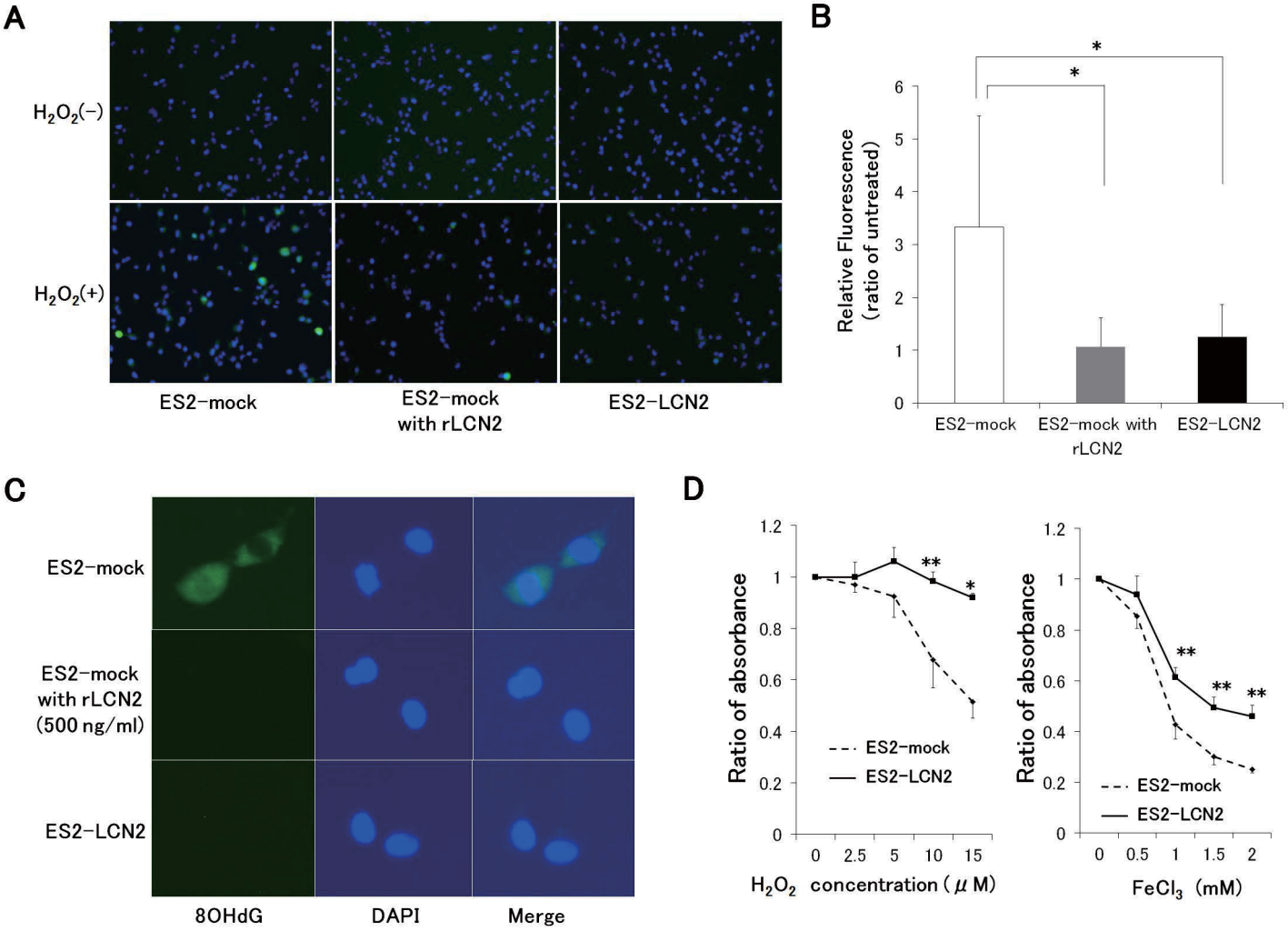
A
$H_2O_2(-)$
$H_2O_2(+)$
ES2−mock
ES2−mock with rLCN2
ES2−LCN2
B
Relative Fluorescence (ratio of untreated)
0
1
2
3
4
5
6
*
*
ES2−mock
ES2−mock with rLCN2
ES2−LCN2
C
ES2−mock
ES2−mock with rLCN2 (500 ng/ml)
ES2−LCN2
8OHdG
DAPI
Merge
D
Ratio of absorbance
1.2
1
0.8
0.6
0.4
0.2
0
**
*
ES2−mock
ES2−LCN2
0
2.5
5
10
15
H_2O_2 concentration (μ M)
Ratio of absorbance
1.2
1
0.8
0.6
0.4
0.2
0
**
**
**
ES2−mock
ES2−LCN2
0
0.5
1
1.5
2
$FeCl_3$ (mM)

Figure 4

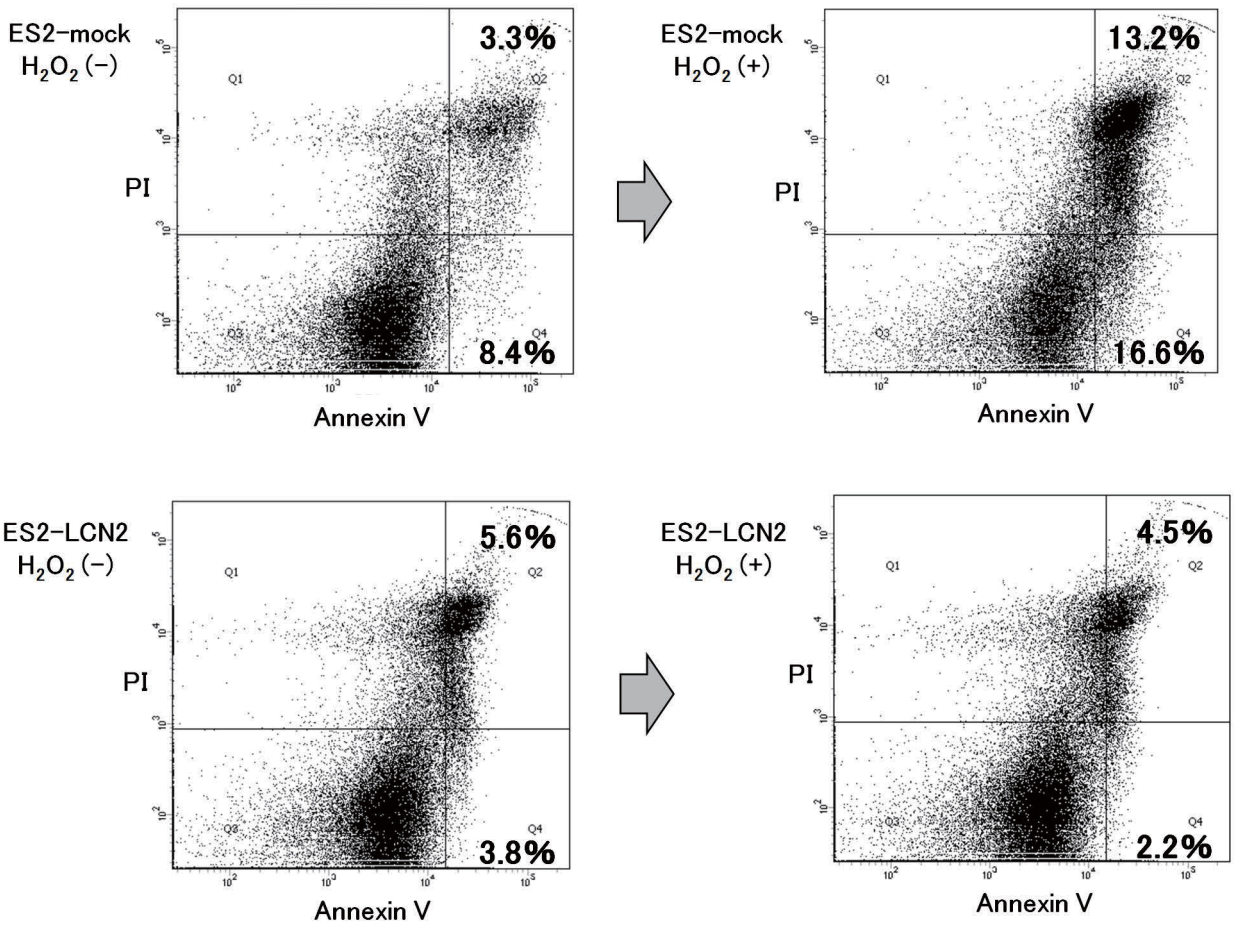
ES2-mock
H2O2 (-)
3.3%
8.4%
PI
Annexin V
ES2-mock
H2O2 (+)
13.2%
16.6%
PI
Annexin V
ES2-LCN2
H2O2 (-)
5.6%
3.8%
PI
Annexin V
ES2-LCN2
H2O2 (+)
4.5%
2.2%
PI
Annexin V

Figure 6

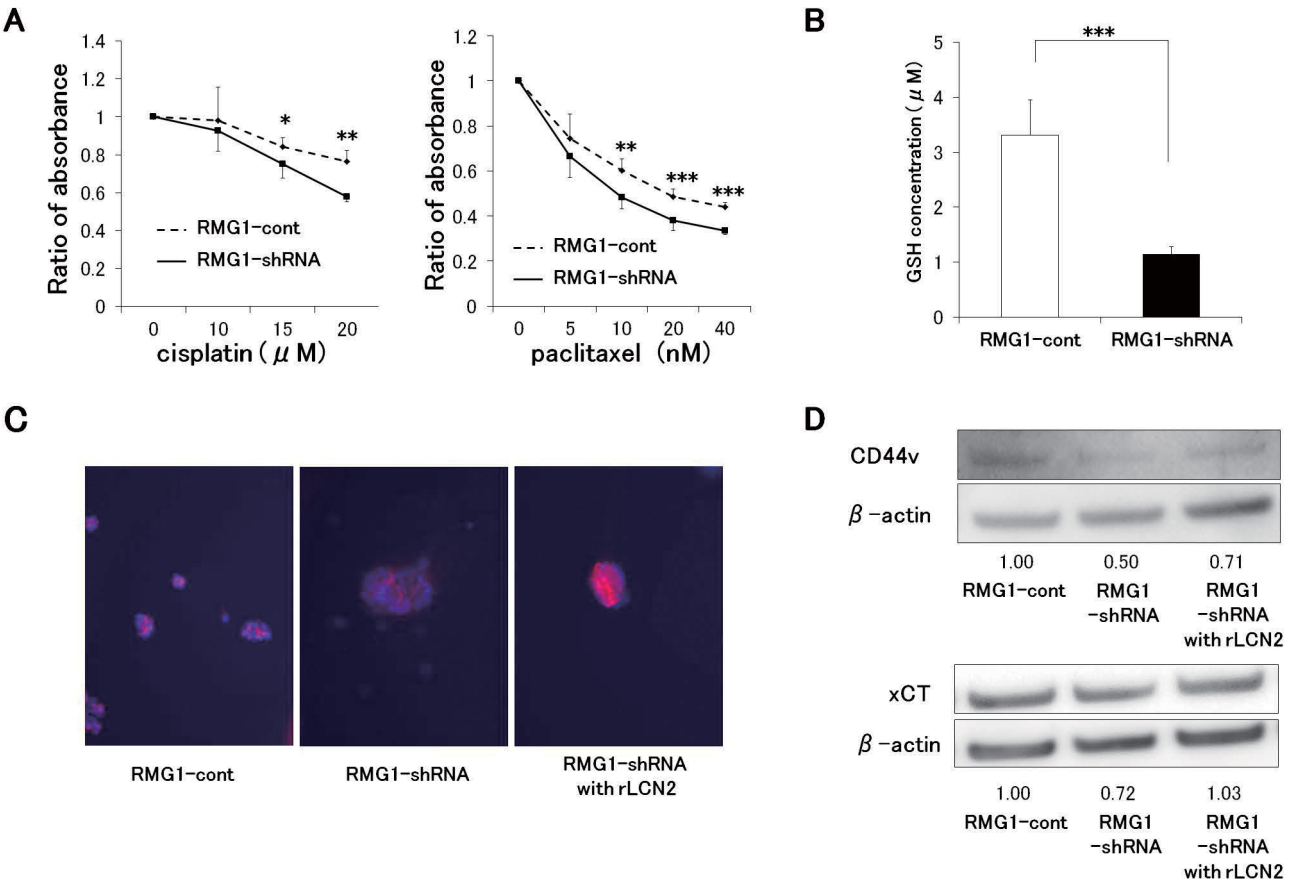
A
Ratio of absorbance
cisplatin (μM)
RMG1-cont
RMG1-shRNA
paclitaxel (nM)
B
GSH concentration (μM)
RMG1-cont
RMG1-shRNA
C
RMG1-cont
RMG1-shRNA
RMG1-shRNA with rLCN2
D
CD44v
β-actin
1.00 RMG1-cont
0.50 RMG1-shRNA
0.71 RMG1-shRNA with rLCN2
xCT
β-actin
1.00 RMG1-cont
0.72 RMG1-shRNA
1.03 RMG1-shRNA with rLCN2

Supplementary figure 1

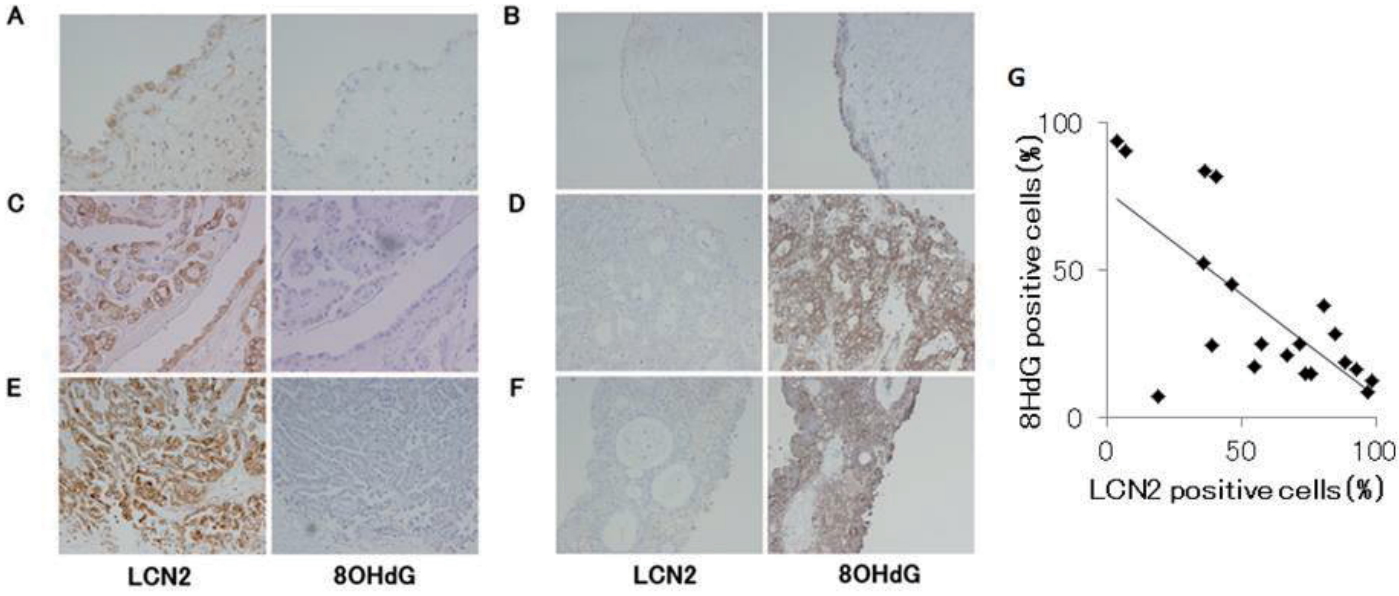

Immunohistochemistry for LCN2 (left) and 8OHdG (right) in ovarian endometriosis (A, B), ovarian clear cell carcinoma (C, D, E), and endometrioid adenocarcinoma (F). 8OHdG expression was increased in lesions that were low expressers of LCN2, and decreased in lesions that were high expressers of LCN2. An inverse correlation was observed between the expression of LCN2 and that of 8OHdG in OCCC (R^2 =0.494, P=0.001) (G).

Supplementary figure 2

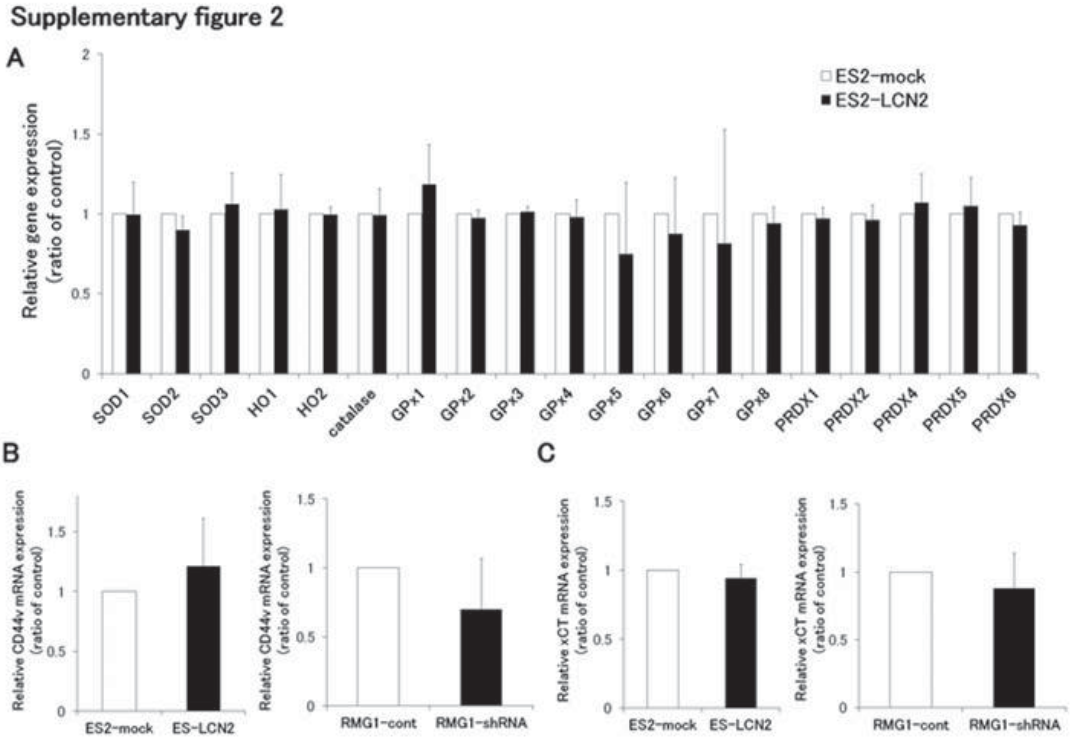

A: Evaluation of mRNA expression of antioxidative enzymes by real-time PCR. The ratio of antioxidative enzymes to β-actin expression was evaluated in ES2-mock and ES2-LCN2 cells. The forced expression of LCN2 did not increase the mRNA expression of antioxidative enzymes. B: Evaluation of CD44v mRNA expression by real-time PCR. The ratio of CD44v mRNA to β-actin expression was evaluated. No significant differences were observed in the expression of CD44v mRNA between ES2-mock and ES2-LCN2 or RMG1-cont and RMG1-shRNA cells. C: Evaluation of xCT mRNA expression by real-time PCR. The ratio of xCT mRNA to β-actin expression was evaluated. No significant differences were observed in the expression of xCT mRNA between ES2-mock and ES2-LCN2 cells or RMG1-cont and RMG1-shRNA cells. Error bars show the standard deviation.

Supplementary figure 3

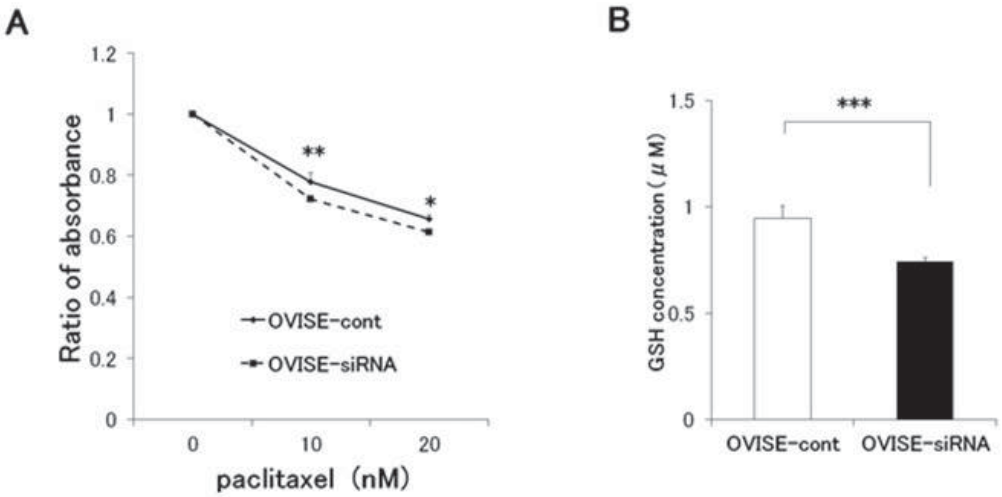

A: Ratio of absorbance in OVISE cells treated with paclitaxel by the WST1 assay. The cell viability of OVISE-cont cells was higher than that of OVISE-siRNA cells. B: Intracellular GSH levels in OVISE cells. Intracellular GSH levels were lower in OVISE-siRNA than that in control cells.
*: < 0.05. **: < 0.01. ***: < 0.001. Error bars show the standard deviation.

Supplementary figure 4

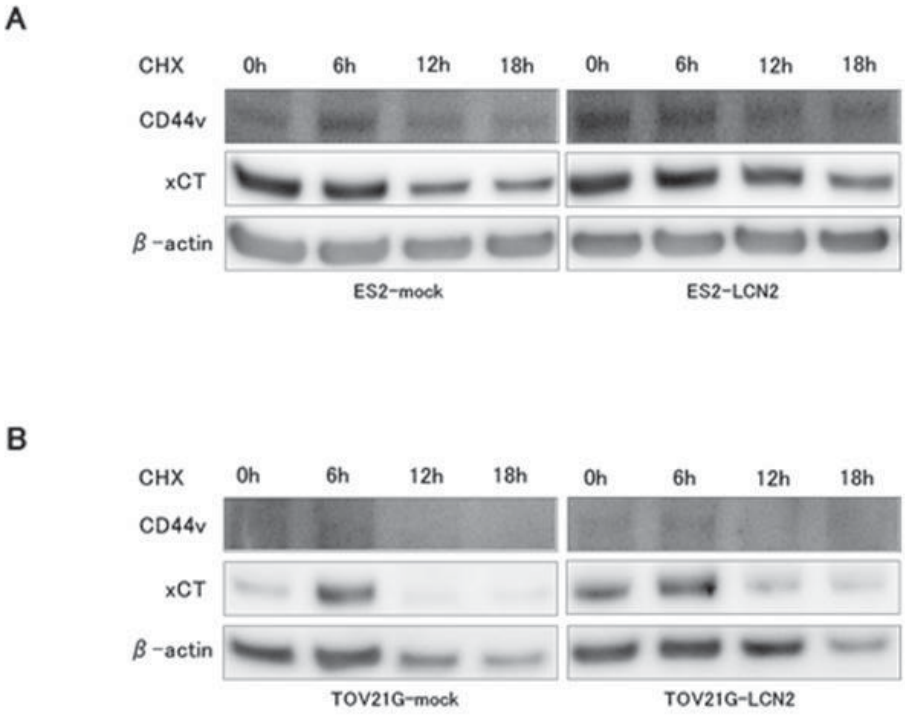

A: CD44v and xCT protein expression in ES2 cells treated with CHX by Western blotting. The degradation of CD44v and xCT was slower in ES2-LCN2 than in ES2-mock cells. B: CD44v and xCT protein expression in TOV21G cells treated with CHX by Western blotting. The degradation of xCT was slower in TOV21G-LCN2 than in TOV21G-mock cells.

Supplementary table 1: Primers for RT-PCR

Gene name	forword	reverse	reference
LCN2	tgtatgccaccatctatgagc	tcctttagttccgaagtcagc	16
b-actin	gacaggatgcagaaggagattact	tgatccacatctgctggaaggt	16
CD44v	agaatccctgctaccaatatggactc	aggtcactgggatgaaggtc	24
xCT	caggagaaagtgcagctgaa	ctccaatgatggtgccaatg	25
SOD1	agggcatcatcaatttcgagc	acattgcccaagtctccaac	
SOD2	ggaagccatcaaacgtgact	ccttgcagtggatcctgatt	
SOD3	atgctggcgctactgtgttc	ctccgccgagtcagagttg	
HO1	atgacaccaaggaccagagc	gtgtaaggacccatcggaga	
HO2	ggaaacctcagaggggtag	gtggccagcttaaacagctc	
catalase	tgaccgagagagaattcctga	cctttgccttggagtatttgg	
GPx1	cagtcggtgtatgccttctcg	gagggacgccacattctcg	
GPx2	gaatgggcagaacgagcatc	ccggccctatgaggaacttc	
GPx3	gagcttgcaccattcggtct	gggtaggaaggatctctgagttc	
GPx4	gaggcaagaccgaagtaaactac	ccgaactggttacacgggaa	
GPx5	atgactacacagttaagggtcgt	ggatattgcgctgtcagacca	
GPx6	caaaggggtaacaggcaccat	ggcggccacattgacaaac	
GPx7	cccaccactttaacgtgctc	ggcaaagctctcaatctcctt	
GPx8	tacttagggctgaaggaactgc	ggctccgattctccaaactga	
PRDX1	cattcctttggtatcagacccg	ccctgaacgagatgccttcat	
PRDX2	gaagctgtcggactacaaagg	tcggtggggcacacaaaag	
PRDX4	agaggagtgccacttctacg	ggaaatcttcgctttgcttaggt	
PRDX5	tctccatggtggtacaggat	gcctcagagctgtgagatg	
PRDX6	gttgccaccccagttgattg	tgaagactcctttcgggaaaagt	
ferritin	cgccagaactaccaccagg	cttcaaagccacatcatcg	
TfR1	ggctacttgggctattgtaaagg	cagtttctccgacaactttctct	